A Proposed Structure for Transmembrane Segment 7 of G Protein-Coupled Receptors Incorporating an Asn-Pro/Asp-Pro Motif

Karel Konvicka, Frank Guarnieri, Juan A. Ballesteros, and Harel Weinstein
Department of Physiology and Biophysics, Mount Sinai School of Medicine, New York, New York 10029, USA

ABSTRACT Transmembrane segment (TMS) 7 has been shown to play an important role in the signal transduction function of G-protein-coupled receptors (GPCRs). Although transmembrane segments are most likely to adopt a helical structure, results from a variety of experimental studies involving TMS 7 are inconsistent with it being an ideal α-helix. Using results from a search of the structure database and extensive simulated annealing Monte Carlo runs with the new Conformational Memories method, we have identified the conserved (N/D)PxxY region of TMS 7 as the major determinant for deviation of TMS 7 from ideal helicity. The perturbation consists of an Asx turn and a flexible "hinge" region. The Conformational Memories procedure yielded a model structure of TMS 7 which, unlike an ideal α-helix, is capable of accommodating all of the experimentally derived geometrical criteria for the interactions of TMS 7 in the transmembrane bundle of GPCRs. In the context of the entire structure of a transmembrane bundle model for the $5HT_{2a}$ receptor, the specific perturbation of TMS 7 by the NP sequence suggests a structural hypothesis for the pattern of amino acid conservation observed in TMS 1, 2, and 7 of GPCRs. The structure resulting from the incorporation of the (N/D)P motif satisfies fully the H-bonding capabilities of the 100% conserved polar residues in these TMSs, in agreement with results from mutagenesis experiments. The flexibility introduced by the specific structural perturbation produced by the (NP/DP) motif in TMS 7 is proposed to have a significant role in receptor activation.

INTRODUCTION

The shared function of all G-protein-coupled receptors (GPCRs) is to transduce an extracellular signal, such as that produced by the binding of a ligand, to the intracellular side by coupling to specific G-proteins (Dohlman et al., 1991; Gudermann et al., 1997). The resulting ternary complex of ligand/receptor/G-protein causes the heterotrimeric G-protein to exchange bound GDP for GTP, and to dissociate into an α-subunit and a β-gamma heterodimer. Both entities are thus enabled to activate intracellular effectors, thereby transducing the signal further downstream and triggering cellular responses such as calcium influx or DNA transcription (Birnbaumer et al., 1990; Clapham, 1996).

The molecular details of the GPCR proteins and of the signal transduction process remain largely unknown because of the difficulties involved in determining the 3D structure of membrane proteins at atomic resolution. Cryo-electron microscopy studies on rhodopsin, a member of the GPCR family, have achieved projections of the electron density map at 7-Å resolution in planes parallel with the membrane (Schertler and Hargrave, 1995; Unger et al., 1997). Theoretical studies based on multiple sequence alignment analysis of hydropathy and amino acid conservation (Ballesteros and Weinstein, 1995; Donnelly et al., 1993) have provided much useful structural information and have led to the construction of different molecular models of GPCRs (Baldwin, 1993; Colson et al., 1998; Findlay et al., 1993; Hutchins, 1994; Laakkonen et al., 1996; MaloneyHuss and Lybrand, 1992; Pogozheva et al., 1997; Strahs and Weinstein, 1997; Trumpp Kallmeyer et al., 1992; Zhang and Weinstein, 1993). Finally, a large array of experiments have probed the structure of the transmembrane domains (for reviews see Baldwin, 1994; Schwartz, 1994; van Rhee and Jacobson, 1996; see also Fu et al., 1996; Javitch et al., 1994, 1995) and have demonstrated structural changes related to function that reflect residue distances (Altenbach et al., 1996; Farahbakhsh et al., 1995; Farrens et al., 1996; Gether et al., 1995, 1997; Resek et al., 1993; Turcatti et al., 1996; Yang et al., 1996).

Individual transmembrane domains of the GPCRs have been identified in many studies as having significant roles in signal transduction. Mutagenesis studies as well as molecular modeling have indicated such a role for transmembrane segment 7 (TMS 7) (Luo et al., 1994; van Rhee and Jacobson, 1996; Wess et al., 1993; Zhang and Weinstein, 1993), with a special contribution from the (N/D)PxxY sequence, which is conserved throughout the GPCR superfamily. Thus mutations of the conserved N or D in this TMS, identified in the universal numbering scheme as 7.49 (see Methods for a description of the numbering system used throughout), or of the conserved P7.50 were shown to perturb significantly the function of the receptors (van Rhee and Jacobson, 1996). Mutations of the tyrosine in the (N/D)PxxY motif, Y7.53, also affect the receptor functions to various extents. Molecular dynamics simulations have identified a possible role for P7.50 in facilitating the specific conformational changes in TMS 7 (Luo et al., 1994; Zhang and Weinstein, 1993) that relate to the various structural rearrangements in the transmembrane region of GPCRs that have been asso-

Received for publication 18 February 1998 and in final form 19 May 1998.
Address reprint requests to Dr. Harel Weinstein, Department of Physiology and Biophysics, Mount Sinai School of Medicine, One Gustave L. Levy Place, Box 1218, New York, NY 10029. Tel.: 212-241-7018; Fax: 212-860-3369; E-mail: hweinstein@msvax.mssm.edu.

0006-3495/98/08/601/11 $2.00

ciated with activation (Altenbach et al., 1996; Ballesteros et al., 1998; Farahbakhsh et al., 1995; Farrens et al., 1996; Gether et al., 1997; Resek et al., 1993; Turcatti et al., 1996; Yang et al., 1996). Consequently, the properties of the Pro-containing TMS 7 that underlie such a dynamic role in signal transduction are of special interest. The helix is generally a rigid structure in a lipid environment, and rhodopsin helices have been proposed to move as rigid domains in the activation process (Farrens et al., 1996), because a break in the structural hydrogen bonds of a helix in a membrane environment would entail an energetically unfavorable exposure of polar groups to the nonpolar medium. Recent results from fluorescence spectroscopy indicate a mechanistic role for the flexibility produced by the prolines in the TMS (Gether et al., 1997). With the (N/D)P conserved sequence in TMS 7, we have identified a particularly flexible hinge region that may play a role in the receptor activation mechanism by functioning as a sensitive conformational switch. The flexibility properties encoded in this motif relate to its special structural characteristics, which produce an energetically favorable local perturbation of the α-helical structure. Notably, a growing number of results from mutagenesis (Liu et al., 1995; Mizobe et al., 1996; Perlman et al., 1997; Rao et al., 1994; Sealfon et al., 1995; Wong et al., 1988; Zhou et al., 1994) and cysteine scanning studies (Fu et al., 1996) of GPCRs are inconsistent with TMS 7 being an ideal α-helix throughout, and suggest structural perturbations that have consequential effects on helix-helix interactions and the packing of the transmembrane helix bundle in GPCRs. A model of TMS 7 incorporating a helix break in the form of a "face-shifted" Pro-kink has been proposed earlier to explain the experimental evidence for departure from ideal α-helical structure (Fu et al., 1996).

We show here that the special structural properties of the conserved (N/D)PxxY motif allow for local flexibility while satisfying the hydrogen bonding requirements of the conserved polar residues in the transmembrane domain of GPCRs. An NP sequence has been identified as an N-cap motif that initiates α-helices from nonhelical structures (Richardson and Richardson, 1988). A Pro residue within an α-helical segment is known to produce a characteristic Pro-kink that disrupts the helical H-bond pattern and causes a bend and a perturbation of the local helical periodicity (Ballesteros and Weinstein, 1992, 1995; Sankararamakrishnan and Vishveshwara, 1992). However, the structure database search we report here shows that when incorporated into α-helical segments, both NP and DP sequences produce structural perturbations that are significantly different from a regular Pro-kink, forming a conformation similar to that of the NP sequence N-cap. Moreover, they appear to induce an unusual degree of structural flexibility. The extensive computational simulations of the (N/D)PxxY segment presented here indicate that the structure identified in the database of soluble proteins for the (NP/DP) sequence can exist in a simulated lipophilic environment. On this basis, the (N/D)PxxY motif in TMS 7 of GPCRs is proposed to adopt a specific structure. This structure can resolve several apparent inconsistencies in the structural interpretation of results from experimental probing of TMS 7 in GPCRs mentioned above, and subserves the functional role attributed to TMS 7 in the activation of GPCRs.

METHODS

Numbering scheme

The generalized numbering scheme (Ballesteros and Weinstein, 1995) that is used throughout is composed of a digit identifying the transmembrane segment (from 1 to 7), and a number associated with a position in the segment relative to the most conserved position in that helix, which is assigned the identifier 50. The other positions are thus numbered relative to this conserved residue with numbers increasing toward the C-terminus and decreasing toward the N-terminus. The general numbering scheme is illustrated on a helical net of a human 5HT2a receptor in Fig. 1.

Sequence alignment

Sequences of GPCRs were retrieved from the Genbank database of nucleotide sequences with STRINGSEARCH from the GCG package (G. C. G., 1996 Wisconsin Package Version 9.0; Madison, WI). Complete genomic sequences and mRNA sequences were translated into protein sequences. The protein sequences were aligned using the PILEUP module of the GCG package. The sequence alignment was searched for duplicate and incomplete sequences, which were deleted. The resulting alignment of 261 GPCRs was refined to extract gaps from proposed transmembrane regions. Analyses of the percentage conservation of amino acids at positions of interest were performed in the alignment.

Search of the protein structure database

The search of the protein structure database was performed with the IDITIS program from Oxford Molecular. The searches for NP and DP sequences contained in a helix were designed in the following manner. First we searched for xNP or xDP surrounded on each side by at least four residues in a helical conformation, where x stands for any residue in any conformation. From the retrieved structures, only nonidentical sequences were selected. The resulting 14 different NP and 16 different DP structures were excised from their original proteins and inspected for conformation. All but one DP structure showed significant disruption of the helical conformation of the segments in which they were imbedded. Only one DP structure was in a regular Pro-kink conformation. Superposition of the helix disruptive NP and DP structures revealed very similar features, as described in the Results.

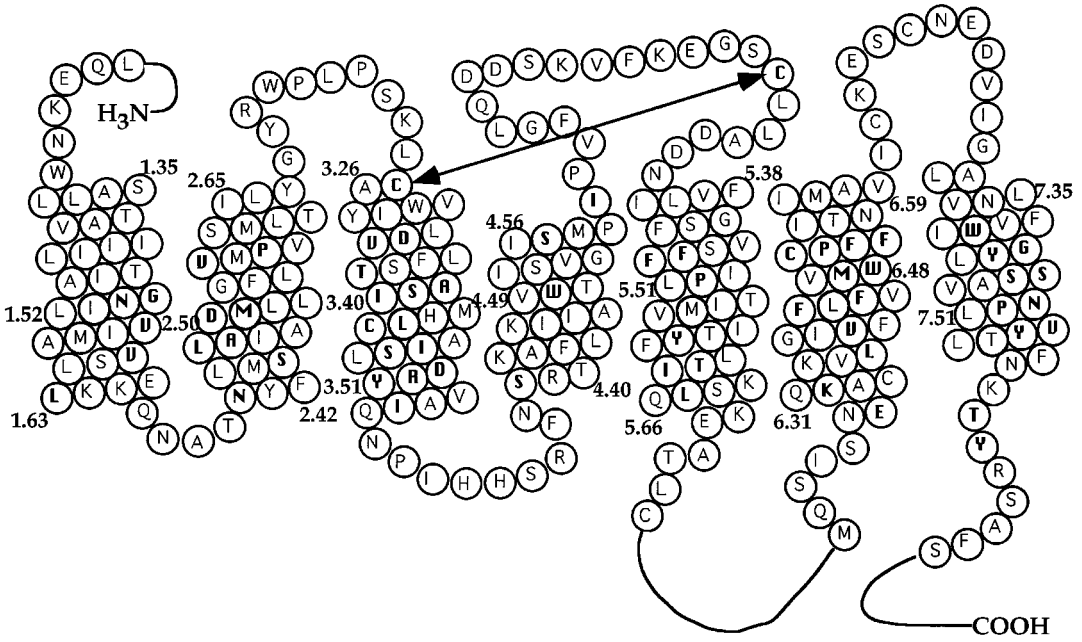

FIGURE 1 Helical net representation of the $5HT_{2a}$ receptor sequence, indicating conserved residues (*in bold*) and the computed ends of TMSs used in the construction of the three-dimensional model.

Conformational Memories procedure

The Conformational Memories technique (Guarnieri and Weinstein, 1996; Guarnieri and Wilson, 1995) was employed to simulate the stretch of TMS 7 between 7.34 and 7.57 with some modifications outlined below.

For the simulation, TMS 7 was divided into three regions: 1) an entirely flexible region extending from Ala 7.47 to Asn 7.49, which included the identified "hinge" region (see Results) and in which both ϕ and ψ backbone dihedral angles and all side-chain χ dihedral angles were varied in the Conformational Memories procedure; 2) two flanking semiflexible boundary regions between Ser 7.45 and Ser 7.46 and between Pro 7.50 and Tyr 7.53, where the rotatable backbone dihedral angles were constrained to $\pm 20°$ around values of -63 and -41.6 for ϕ and ψ dihedral angles, respectively, and all side-chain χ dihedral angles were left to rotate freely; and 3) the intracellular and extracellular ends of TMS 7, which were kept rigid. The dihedral angles defining the starting conformations are specified in Table 1. The entire Conformational Memories procedure was carried out in the chloroform solvent model environment (Still et al., 1990), using the AMBER* forcefield (McDonald and Still, 1992) implemented in MACROMODEL (Mohamadi et al., 1990).

The Conformational Memories procedure consisted of four steps:

First, a classical Metropolis Monte Carlo (Metropolis et al., 1953) (MC) simulation was performed in torsion space at 10,000K for 1,000,000 steps, depositing 64 structures evenly spaced along the simulation. Two simulations starting from two different starting structures (the conventional Pro-kink and the NP/DP motif identified from the database search) were performed in parallel, resulting in a collection of two sets of 64 structures.

In the second phase, a simulated annealing from 10,000K to 582K was performed on both sets of 64 structures, monitoring every step of the Metropolis MC simulation. The cooling schedule followed a formula $T_{n+1} = T_n * 0.9$, which resulted in 28 temperatures, with 10,000 steps of Metropolis MC performed at each temperature. At each Metropolis MC step, two new values for two dihedral angles were selected randomly from an interval of $\pm 180°$ around the previous values of the dihedral angles, except for the constrained backbone dihedral angles of the boundary regions, which were selected from an interval of $\pm 20°$. The two parallel simulations starting from the NP/DP motif and the Pro-kink provided two separate sets of dihedral angle population maps, as described by Guarnieri and Weinstein (1996). Notably, the two sets did not differ significantly, demonstrating the convergence of the conformational space exploration (see Results).

In the third phase, two biased Metropolis MC simulations were performed using the set of populations obtained from all data. At each biased Metropolis MC step, three randomly selected dihedral angles were assigned a new value as described previously (Guarnieri and Weinstein, 1996; Guarnieri and Wilson, 1995), using a new biased temperature annealing method (Guarnieri, unpublished observations), which incorporates temperature variation into the biased sampling. Biased temperature annealing enables conformational sampling by overcoming the very high barriers that exist between the Pro-kink and NP/DP motif structures. Thus 50 of these biased annealings were performed from 1000K to 310K in 12 temperature steps, following the

TABLE 1 Dihedral angles defining the starting structures for the MC procedure

	ϕ		ψ		χ_1		χ_2	
Residue	Pro-kink	NP/DP model	Pro-kink	NP/DP model	Pro-kink	NP/DP model	Pro-kink	NP/DP model
A7.33	−63.0	−63.0	−41.6	−41.6				
L7.34	−63.0	−63.0	−41.6	−41.6	180	180	180	180
L7.35	−63.0	−63.0	−41.6	−41.6	180	180	180	180
N7.36	−63.0	−63.0	−41.6	−41.6	180	180	−90	−90
V7.37	−63.0	−63.0	−41.6	−41.6	180	180		
F7.38	−63.0	−63.0	−41.6	−41.6	180	180	90	90
V7.39	−63.0	−63.0	−41.6	−41.6	180	180		
W7.40	−63.0	−63.0	−41.6	−41.6	180	180	−82.8	−82.8
I7.41	−63.0	−63.0	−41.6	−41.6	−60	−60	180	180
G7.42	−63.0	−63.0	−41.6	−41.6				
Y7.43	−63.0	−63.0	−41.6	−41.6	180	180	90	90
L7.44	−63.0	−63.0	−41.6	−41.6	180	180	180	180
S7.45	−63.0	−63.0	−41.6	−41.6	−60	−60		
S7.46	−63.0	−63.0	−41.6	−41.6	−60	−60		
A7.47	−68.9	−68.9	−37.9	−37.9				
V7.48	−75.8	67.0	−42.6	−105.1	180	180		
N7.49	−55.3	−160.0	−50.6	134.0	180	180	−90	−90
P7.50	−57.2	−57.2	−43.9	−43.9	−17.1	−17.1	31.2	31.2
L7.51	−63.0	−63.9	−41.6	−41.6	180	180	180	180
V7.52	−63.0	−73.3	−41.6	−41.6	180	180		
Y7.53	−63.0	−60.1	−41.6	−41.6	180	180	90	90
T7.54	−63.0	−63.0	−41.6	−41.6	−60	−60		
L7.55	−63.0	−63.0	−41.6	−41.6	180	180	180	180
F7.56	−63.0	−63.0	−41.6	−41.6	180	180	90	90

temperature schedule of $T_{n+1} = T_n$*0.9. At each temperature 10,000 biased Metropolis MC steps were performed, except for 20,000 steps at 310K, during which two structures were collected, each after 10,000 steps. Therefore, each of the two separate runs resulted in a collection of 100 structures.

In the fourth and final phase, the two sets of 100 structures were clustered into families using the program XCLUSTER (Shenkin and McDonald, 1994). The selection was based on root mean square differences of all heavy atoms after superposition. Individual members of the resulting families had root mean square differences of less than 1.09 Å.

The $5HT_{2a}$ receptor model

A model of the transmembrane part of the $5HT_{2a}$ receptor was constructed following the considerations outlined in a recent review (Ballesteros and Weinstein, 1995). The ends of individual TMSs were determined from computed periodicity profiles of hydrophobicity, conservation of amino acid volume, and amino acid conservation, extracted from a GPCR alignment, and the helices were organized according to the template of the cognate rhodopsin molecule (Baldwin et al., 1997; Schertler and Hargrave, 1995; Unger et al., 1997). The relative orientations and interactions between the helices were adjusted based on conservation of amino acid properties such as hydrophobicity, polarity, aromatic character, etc. (for a recent review of this approach see Ballesteros and Weinstein, 1995), and incorporated structural inferences from available experimental data, such as mutation and ligand binding experiments (Baldwin, 1994; Schwartz, 1994; van Rhee and Jacobson, 1996), cysteine scanning data (Fu et al., 1996; Javitch et al., 1994, 1995), and interactions and proximities suggested from electron paramagnetic resonance (Farrens et al., 1996), cysteine cross-linking (Yu et al., 1995), engineering of zinc binding sites (Elling et al., 1995; Elling and Schwartz, 1996; Sheikh et al., 1996), and mutation experiments (Liu et al., 1995; Perlman et al., 1997; Rao et al., 1994; Sealfon et al., 1995; Zhou et al., 1994). The complete details of the resulting $5HT_{2a}$ receptor model construction will be discussed elsewhere.

The minimization of the $5HT_{2a}$ receptor model of the transmembrane bundle was performed using CHARMM 24 (Brooks et al., 1983) with Charmm 22 parameters in three steps. In the first step all C_α-carbons in TMS 1–6 were fixed, and the backbone dihedral angles of TMS 7 were constrained, except for the "hinge" region consisting of ϕ and ψ dihedrals of Val 7.48 and the ϕ dihedral angle of Asn 7.49. H-bonding distances between residues Asn 1.50, Asp 2.50, Asn 7.49, and exposed backbone polar groups of TMS 7 were constrained at 1.7 Å (H - heavy atom distance) with 11 harmonic distance constraints. One thousand steps of adopted-basis Newton-Raphson minimization were performed. In the second step, all of the constraints except the 11 harmonic distance constraints were removed, and 1000 steps of adopted-basis Newton-Raphson minimization were performed. In the last step, the remaining constraints were released and 1000 steps of minimization were applied.

RESULTS

Structure database search

The (N/D)P sequence in TMS 7 is 100% conserved in GPCRs in a structural environment considered to be helical. A search of the structure database (Abola et al., 1987; Bernstein et al., 1977) identified 14 NP and 16 DP sequences flanked by helices on either side. Of these, 14 NP and 15 DP retrieved structures adopt a conformation that is significantly different from the Pro-kink expected in a proline containing helix (Ballesteros and Weinstein, 1992, 1995; Sankararamakrishnan and Vishveshwara, 1992). In the only DP sequence found in the Pro-kink conformation (in pdb1atr.ent), the Asp side chain appears to be stabilized in the helical conformation by a patch of adjacent positively charged residues. All of the other structures were characterized by a break in the helix displaying a set of common features. Thus the carbonyl group of the Asn or Asp side chain in all of these structures forms a hydrogen bond with a backbone NH group of the residue at position $i + 1$ and/or $i + 2$ (relative to the Pro at position i). It appears that this characteristic Asx turn, together with the Pro, stabilizes the N-terminus of the continuing helix after the (N/D)P break. To achieve the characteristic side chain–backbone interaction, the Asx backbone dihedral angle ψ value must lie around 100°, as shown in Fig. 2. This dihedral angle is significantly different from ψ in a helical segment; more importantly, it would generate a steric clash with the helix backbone for residues in an α-helix or even at the position $i - 1$ in a Pro-kink. The (N/D)P motif connects the preceding and following helical segments with a short hinge that allows the two helices to be positioned in an orientation that depends on the rest of the tertiary structure. The resulting hinge is likely to be flexible, as indicated by the wide spread of dihedral angle values found in the structures identified in the search (Fig. 2). The flexibility is achieved through rotations around the backbone dihedral angle ϕ of Asx_{i-1}, and around the two backbone dihedral angles ϕ and ψ of the residue at position $i - 2$ and, to a lesser extent, of the residue at $i - 3$. This type of helix structure, specifically broken in the neighborhood of the Pro, was also proposed from NMR experiments performed on the isolated TMS 7 of the tachykinin NK-1 receptor (Berlose et al., 1994).

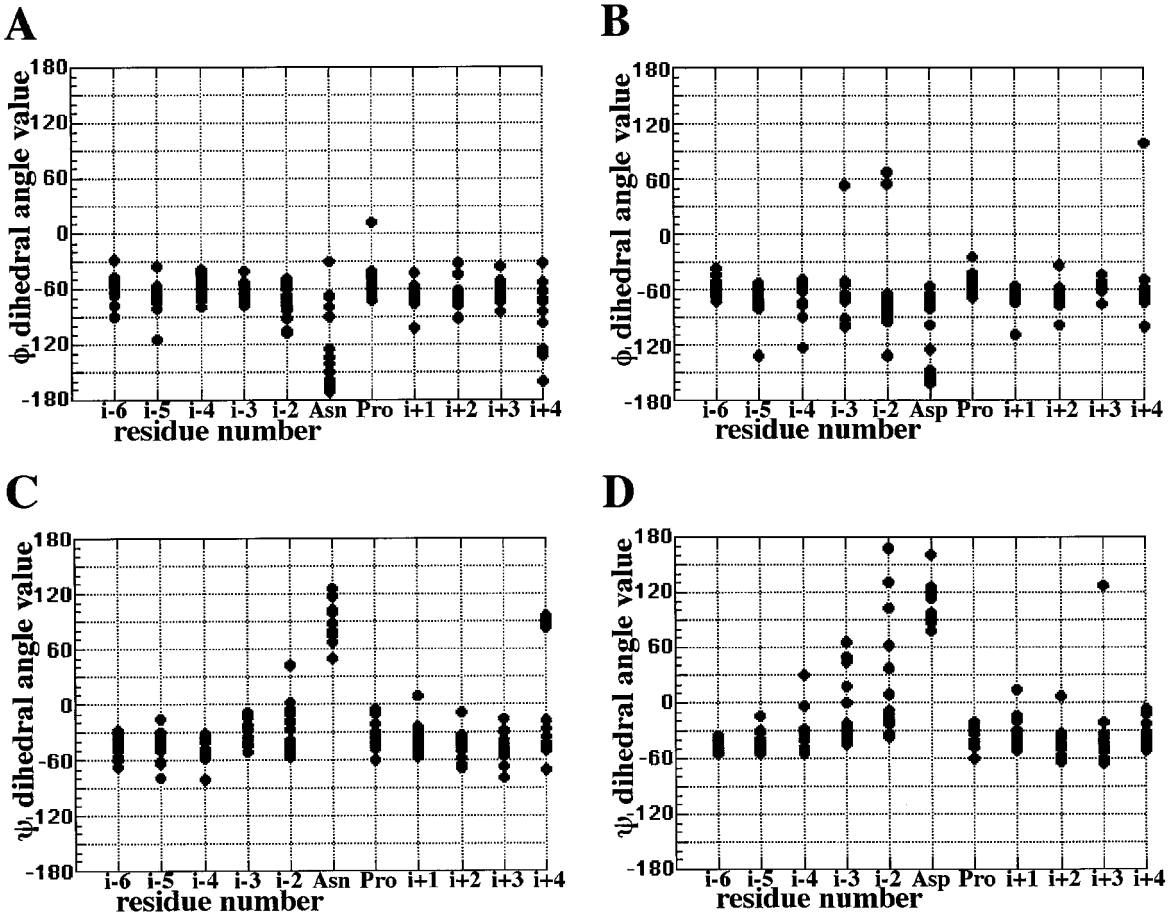

FIGURE 2 Plots of ϕ and ψ backbone dihedral angles of structures retrieved from the database search. Data are given for the 14 NP-containing structures and the 15 DP-containing structures retrieved from the search, in the region of residues $i - 6$ to $i + 4$, where i denotes the position of Pro. Note the nonhelical values of ψ dihedral angles of N_{i-1} or D_{i-1} that show a spread around 100°. (*A* an *B*) Distribution of ϕ dihedral angles of structures containing (*A*) the NP sequence and (*B*) the DP sequence. (*C* and *D*) Distribution of *y* dihedral angles of structures containing (*C*) the NP sequence and (*D*) the DP sequence.

Conformational preferences of the NPxxY region

To evaluate the conformational preferences of the NPxxY region of TMS 7 of GPCRs in a hydrophobic environment, extensive Conformational Memories simulations were carried out as described in Methods, using a continuum chloroform solvent model (Still et al., 1990). A model of TMS 7 of the $5HT_{2a}$ receptor was constructed by incorporating the (N/D)P sequence characteristics identified with the structure database search described above. Both this initial model based on the results from the structure database search for (N/D)P sequence properties (the "NP/DP initial model") and a regular Pro-kink structure of $5HT_{2a}$ receptor TMS 7 were used as starting points for identical sets of calculations, as described in Methods. It has recently been demonstrated that the technique of Conformational Memories is capable of performing a complete rapid search of a hyperdimensional conformational space, producing a Boltzmann distribution of structures (Guarnieri and Weinstein, 1996; Guarnieri and Wilson, 1995). The convergence of the conformational space exploration applied here was checked by careful criteria at every step of the procedure, as described below.

Each set of 64 different structures, resulting from two constant temperature Metropolis MC simulations at 10,000K starting from Pro-kink and NP/DP initial model structures as described in Methods, was annealed from 10,000K to 582K, producing population maps for all of the dihedral angles that were allowed to rotate in the Conformational Memories simulations. The high temperature of 10,000K produced interconversion between available minima. The annealing was stopped at 582K, because below 1000K we observed a 0% acceptance ratio. Population maps for all simulated dihedral angles were obtained from the two sets of 64 annealings.

The resulting dihedral angle populations did not differ significantly between the two sets started from a regular Pro-kink and the NP/DP initial model, respectively. Because the parallel runs were started from such very distinct starting structures, the convergence of the population map indicates the completeness of the conformational space exploration.

The biased simulated annealing expedites the exploration of the conformational space (Guarnieri and Weinstein, 1996; Guarnieri and Wilson, 1995). The acceptance ratio is enhanced to ~9% at 1,000K, which is the highest temperature used in the biased simulated annealing, and to ~1% at 310K. This procedure allowed us to obtain a structure distribution at the biologically relevant temperature of 310K. The biased simulation was launched separately for the NP/DP initial model and the Pro-kink structures to test again the convergence of the conformational space exploration. Each of the two runs (see Methods) resulted in a collection of 100 structures that were separately assembled into families of similar structures.

As was the case for the population maps, the structure distributions resulting from the biased simulated annealing procedure were also very similar for simulations starting from either the NP/DP initial model or the Pro-kink structures. Because the starting structures differ significantly in many dihedral angle values, the convergence of the procedure to one common set of structural families is an indication that the entire conformational search has converged. Moreover, the individual structures that compose the major structural families did not appear in separate clusters, but were dispersed throughout the simulation, further indicating interconvergence among the families within each run. The family interconvergence substantiates the calculated percentages of family populations (see below).

Most importantly, the Conformational Memories simulation procedure showed that in the hydrophobic environment mimicked by the chloroform solvent model, the NP sequence breaks the helix structure of TMS 7 in a way similar to that identified from the structure database search for (N/D)P structures described above. The Conformational Memories conformational search identified two major structural families for the isolated TMS 7 of the $5HT_{2a}$ receptor. Both of these families incorporate the Asx turn, which locally disrupts the helicity.

A final model structure for TMS 7 was selected from the results of these simulations based on the following selection criteria. First, the two helical parts of the TMS 7, before and after the NP, must be in an orientation that is close to parallel to allow TMS 7 to span the membrane and to permit efficient packing with the neighboring TMSs. Second, the relative rotational orientation of the two helix parts must create a distribution of residues on TMS 7 that can accommodate the inferences about proximities and helix-helix interactions probed experimentally (Fu et al., 1996; Liu et al., 1995; Mizobe et al., 1996; Perlman et al., 1997; Rao et al., 1994; Sealfon et al., 1995; Wong et al., 1988; Zhou et al., 1994).

The major conformational family represents 83% and 72% of the structures in simulations starting from the NP/DP initial model structure and the Pro-kink structure, respectively. This major family does not comply with the first selection criterion because it incorporates a ~90° turn around the NP-motif, making it unlikely to exist in a helical bundle (Fig. 3).

The second major family represents 15% and 24% of the populations resulting from simulations starting with the NP/DP initial model and Pro-kink structures, respectively. In this family, the extracellular and intracellular helical parts of the TMS 7 are at an angle of >135°, satisfying the first selection criterion. The overall structure allows reasonable packing with other TMSs in the transmembrane bundle (Fig. 4). The shifted face of the helix above the NP7.50 relative to the helix below the NP7.50 accommodates the interactions proposed from experimental results, satisfying the second selection criterion.

A prominent structural feature of this family is a hydrogen bond interaction between the conserved Tyr 7.53 and a backbone carbonyl of residue 7.47 at the end of the extracellular helical part (Fig. 4). The conserved Tyr 7.53 may

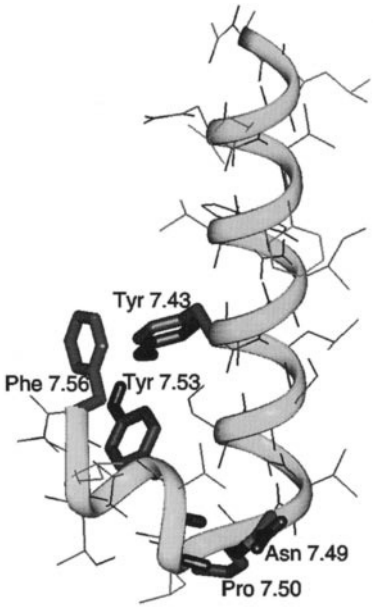

FIGURE 3 A representative structure selected from the largest structural family resulting from the MC procedure. The angle between the extracellular and intracellular helical parts of this putative TMS 7 would not permit spanning of the membrane and reasonable packing with other TMSs.

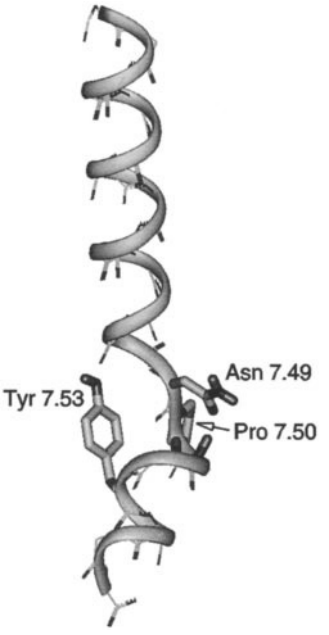

FIGURE 4 The model structure of TMS 7 resulting from the MC procedure and used in the $5HT_{2a}$ receptor transmembrane bundle.

therefore play a role in stabilizing the particular conformation of the flexible region defining the relative positioning of the helices above and below the NP7.50. The dihedral angles defining the conformation of the NP7.50 and its neighborhood are specified in Table 2. This conformational family appeared to be an excellent candidate for the TMS 7 structure, and a representative structure was selected as an initial structure for TMS 7 in modeling the transmembrane bundle.

Incorporation of the proposed structure of TMS 7 into a model of the transmembrane domain

The model structure of TMS 7 was incorporated into a model of the $5HT_{2a}$ receptor transmembrane bundle to investigate possible interactions with the neighboring TMSs. The position of TMS 7 in the bundle was determined by considering both conservation information extracted from a sequence alignment and experimental data from mutagenesis (van Rhee and Jacobson, 1996) and cysteine scanning experiments (Fu et al., 1996). Thus TMS 7 was oriented so that the face with conserved residues and with residues accessible to polar Cys probes is positioned inside the core of the transmembrane bundle (Fu et al., 1996). This positioning was further refined using a set of interactions proposed experimentally between residues in TMS 7 and TMS 1 (Liu et al., 1995), TMS 1 and/or 2 (Mizobe et al., 1996), TMS 2 (Perlman et al., 1997; Sealfon et al., 1995; Zhou et al., 1994), TMS 2 and 3 (Rao et al., 1994), TMS 3 (Oprian, 1992), and TMS 3 and/or 6 (Mizobe et al., 1996). All of these interactions can be satisfied without conflict when the TMS 7 model proposed here was used, but could not all be satisfied with TMS 7 modeled as a regular helix. This is illustrated in Fig. 6. Note the repositioning of the Asn 7.49 closer to TMS 2 for the proposed interaction with Asp 2.50 as compared to a regular helix described in Fig. 5. The repositioning occurred as a consequence of the NP structural perturbation and the ensuing rotation of the helices above and bellow the NP7.50 with respect to each other.

Because earlier work showed that polarity conserved positions cluster together in the cores of proteins to create conserved hydrogen bonding interactions (Zhang and Weinstein, 1994), we refined the model by energy minimization as described in Methods, while restraining the proximity of the conserved polar residues 7.49, 2.50, and 1.50 in accordance with data from site-directed mutagenesis (Perlman et al., 1997; Sealfon et al., 1995; Zhou et al., 1994). The resulting model fulfills all of the constraints and proposed interactions identified above, as depicted in Fig. 6. Notably, a hydrogen bond network was formed among the conserved polar residues after the minimization. The Tyr 7.53 in the unconstrained part of the minimization switched to H-bond the side chain CO group of the Asn 1.50, and Asn 1.50 replaced the H-bond interaction of the Tyr 7.53 with the backbone CO group of residue 7.47. This interaction rearrangement allowed for parallel alignment of the two helical segments of TMS 7 and thereby for very efficient packing with other TMSs. In this minimized model, Asp 2.50 forms hydrogen bonds with both Asn 1.50 and Asn 7.49. The 100% conserved polar residues, Asn 1.50, Asp 2.50, and Asn 7.49, are thus fully saturated with H-bonds to each other and to other conserved polar groups in the model. This H-bond network suggests a structural explanation for the

TABLE 2 Dihedral angle values defining the NP/DP model structure resulting from the MC procedure

Residue	S7.45	S7.46	A7.47	V7.48	N7.49	P7.50	L7.51	V7.52	Y7.53
Dihedral									
ϕ	−64.7	−58.4	−55.4	−97.4	−125.8	−57.2	−63.9	−73.3	−60.1
ψ	−41.3	−45.4	−22.6	62.5	111.6	−35.0	−24.6	−49.2	−38.8
χ_1	−50.1	−53.6		−162.4	175.5	−17.1	174.1	161.3	−46.0
χ_2					−9.5	31.2	170.0		123.1

Only dihedral angles varied in the procedure are included; the N- and C-terminal ends of TMS 7 remain as defined in the starting structures.

conservation of the polar residues at positions 1.50, 2.50, 7.49, and 7.53 (see below).

DISCUSSION

Results from a large variety of studies suggest that TMS 7 plays a major role in GPCR function (Luo et al., 1994; van Rhee and Jacobson, 1996; Wess et al., 1993; Zhang and Weinstein, 1993). A TMS 7 in an ideal α-helix conformation is inconsistent with a number of interactions between residues on TMS 7 and surrounding TMSs that were inferred from various experiments (Liu et al., 1995; Mizobe et al., 1996; Perlman et al., 1997; Rao et al., 1994; Sealfon et al., 1995; Wong et al., 1988; Zhou et al., 1994). The discrepancies (depicted in Fig. 5) have been noted recently by Fu et al. (1996), and a model structure has been proposed to reconcile the experimental data. The proposed model structure contains a perturbation at the position of the Pro 7.50 in a form of a highly pronounced Pro-kink. Our present findings also suggest a significant perturbation in the helicity of the TMS 7, which incorporates here a motif structure adopted by most NP and DP sequences in soluble proteins. The model structure resolves the structural incompatibilities with α-helical models outlined above, and in addition imparts to the transmembrane region a degree of flexibility that is likely to be important in the signal transduction process. It is possible, therefore, that TMS 7 adopts different conformations in different functional states of the receptor.

The specific structural features of the perturbation in the resulting model of TMS 7 that were identified from Conformational Memories simulations in a hydrophobic environment are consistent with the results of the PDB search for NP/DP sequences in helices of soluble proteins and with the conservation of the (N/D)PxxY sequence in TMS 7 of GPCRs. Notably, the result is very similar in the NP region to the NMR proposed structure for tachykinin NK-1 receptor TMS 7 measured in isolation (Berlose et al., 1994). However, because of the H-bond established between the side chain of Tyr7.53 and the backbone carbonyl of residue 7.47 at the end of the extracellular helical part of TMS 7, the

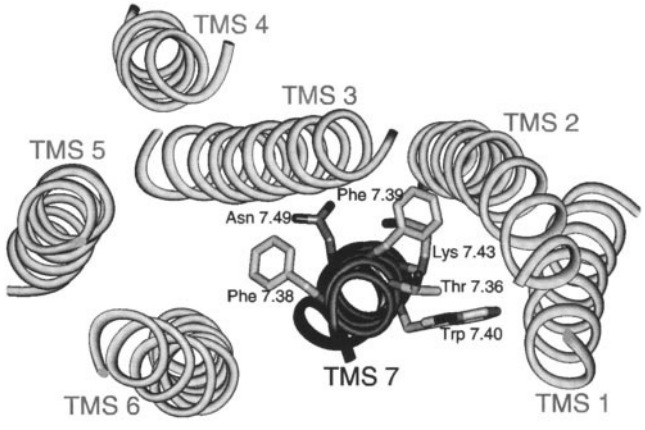

FIGURE 5 Schematic representation of the transmembrane (TM) region of GPCRs that is incompatible with all experimental data. Transmembrane segments (TMSs) are represented by ideal α-helices incorporating Pro-kinks around conserved Pro positions. The view is from the extracellular side. TMS 7 shows residues from various receptors that help position the TMS 7 according to the proposed interactions and proximities. Thr 7.36 was proposed to interact with TMS 1 (Liu et al., 1995), and Phe 7.38 and 7.39 were proposed to interact with TMS 3 and/or 6 and TMS 1 and/or 2, respectively (Mizobe et al., 1996). Trp 7.40 needs to face the interior of the TM bundle, because it was labeled by photoaffinity-activated ligand (Wong et al., 1988). Lys 7.43 connects the retinal molecule in rhodopsins through the Schiff base and is neutralized by counterions in either TMS 3 (wild type) (Oprian, 1992) or TMS 2 (Rao et al., 1994). Asn 7.49 was proposed to interact with Asp 2.50 in $5HT_{2a}$ (Sealfon et al., 1995), GnRH (Zhou et al., 1994), and TRH (Perlman et al., 1997) receptors. Note that when the interactions above the Asn 7.49 are satisfied, the Asn 7.49 in the ideal α-helix model of TMS 7 is too distant from TMS 2 to engage in the proposed interaction.

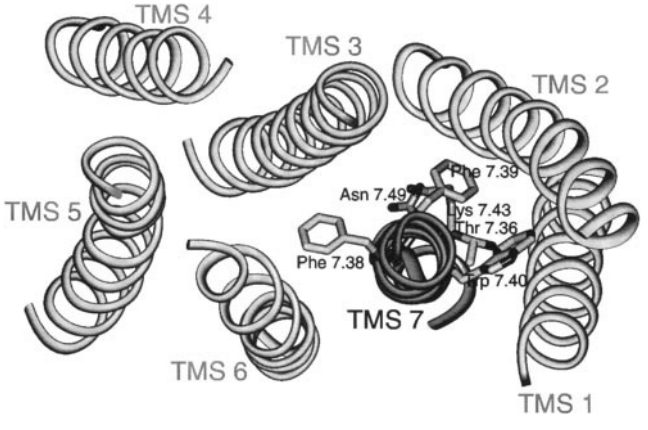

FIGURE 6 Model structure of the TM part of the $5HT_{2a}$ receptor incorporating the model of TMS 7 resulting from the MC procedure. Note that the interactions and proximities discussed in Fig. 5 can be incorporated simultaneously without a conflict. The TM helices are represented with a ribbon, and some of the key residues in TMS 7 are shown as they are in other receptors to illustrate the feasibility of the proposed interactions in these receptors (see legend of Fig. 5 for specific references). Thus residues Asn 7.36, Val 7.39, and Tyr 7.43 were replaced with Thr, Phe, and Lys, respectively, for this illustration.

computer-generated structure seems to have the two helical parts oriented more parallel than the proposed NMR structure.

The structural characteristics identified here for the (N/D)PxxY motif in TMS 7 play a key role in integrating the available structural inferences about the transmembrane bundle (cf. Figs. 5 and 6). It is noteworthy that the H-bonding capabilities of the conserved polar residues at positions 1.50, 2.50, 7.49, and 7.53 are fully saturated in this model (for the H-bond network see Fig. 7). This is in agreement with the demonstrated propensity of polar residues buried inside the soluble proteins to be stabilized by formation of H-bonds with other buried polar groups so that only ~5% of polar groups are unsatisfied in their H-bonding potential (McDonald and Thornton, 1994).

Through this H-bonding network, the perturbation of the helix in the NP region of TMS 7 offers a structural explanation for the conservation profile of the neighboring TMSs in the neighborhood of the NP7.50. An especially strong reason appears for the Asn 1.50 to be conserved, as this residue helps to adjust the two helical parts of TMS 7 in a more parallel orientation than in the structure resulting from the Conformational Memories procedure, by H-bonding the Tyr 7.53 and the backbone carbonyl exposed by the NP perturbation. The parallel orientation is favorable for the packing to the other TMSs. By H-bonding the Tyr 7.53, the Asn 1.50 also stabilizes the rotational reorientation of the intracellular helical part of the TMS 7 relative to the extracellular part, which allows for the experimentally identified interaction between Asn 7.49 and Asp 2.50. This may also explain the conservation of the Tyr 7.53, because no other residue presenting an H-bond donor could reach the Asn 1.50.

The importance of the saturated H-bonding network appears to be supported further by a group of conserved hydrophobic residues situated below the conserved polar residues in TMS 1, TMS 2, and TMS 7 at positions 1.53, 1.54, 2.46, 2.42, 3.46, 7.51, and 7.52 that was identified from the sequence alignment analysis. As illustrated in the model, these residues may form an interlaced hydrophobic cluster underlying the polar H-bond network that could screen it from the intracellular polar environment (Fig. 8). Notably, the participating Leu 2.46 is highly conserved, creating the LxxxD sequence motif in TMS 2. Our model suggests that the high conservation at this position is due to the direct packing of Leu 2.46 against Asp 2.50 and Asn 7.49, and that a substitution by a β-branched residue such as Val or Ile or by a polar residue would perturb the H-bond interaction. Position 7.52 has a very high occurrence of Ile (59%) and is 87% conserved Ile/Val/Leu. If TMS 7 were an ideal α-helix, position 7.52 would face the membrane, and the high content of Ile would not appear to have any structural role. In our model, however, the residue packs directly against the side chain of Asn 1.50 from the intracellular side, supporting the H-bond network. Absence of polar residues at these positions in the alignment supports the hypothesis of a hydrophobic screening function for the hydrophobic cluster created by these residues; substitution at any of these positions by a polar residue is likely to interfere directly with the conserved H-bond network.

The conjectured need for structural flexibility in the function of the transmembrane domain of GPCRs (Luo et al., 1994) is supported by the perturbation produced by the (N/D)PxxY sequence in the helical structure of the TMS 7. A large movement at the intracellular side of the TMS 7 is likely to be achieved by small repositioning of the H-bond network, especially the H-bond acceptors interacting with Asn 7.49. An increased distance between the intracellular ends of TMS 1 and 7 upon activation has been measured experimentally (Hubbell et al., 1995). Because the conserved H-bond network is screened by a hydrophobic cluster only from the intracellular side, direct or indirect ligand interference with the H-bonds that would produce the rear-

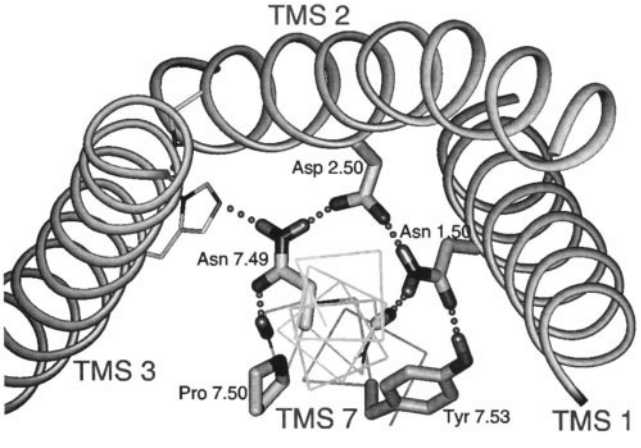

FIGURE 7 The H-bond network between the conserved Asn 1.50, Asp 2.50, Asn 7.49, and Tyr 7.53 established in the $5HT_{2a}$ receptor model. Note the H-bond saturation of the conserved residues, which was made possible by the perturbation in TMS 7. Also note that the perturbation causes a rotation of the position of the Tyr 7.53 with respect to the intracellular helical part of TMS 7; the rotation makes possible the H-bond interaction of the Tyr 7.53 with Asn 1.50.

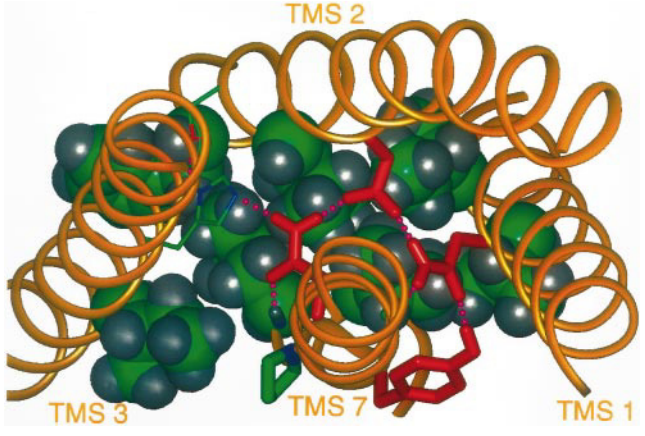

FIGURE 8 The cluster of hydrophobic residues is screening the H-bond network established by TMS 7 from the intracellular polar environment. The view is from the extracellular side.

rangement around the flexible hinge is facilitated. This facilitated rearrangement, supported by the perturbation of helical structure, involves the residues in positions 2.50 and 7.49 that have been shown to be essential for receptor function (Ballesteros et al., 1998; Perlman et al., 1997; Sealfon et al., 1995; van Rhee and Jacobson, 1996; Zhou et al., 1994).

This work was supported by National Institutes of Health grants R01-DK46943, T32-DA07135, R01-DA09083, and K05-DA00060.

REFERENCES

Abola, E. E., F. C. Bernstein, S. H. Bryant, T. F. Koetzle, and J. Weng. 1987. Protein Data Bank in Crystallographic Databases—Information Content, Software Systems, Scientific Applications. Data Commission of the International Union of Crystallography, Bonn, Cambridge, and Chester.

Altenbach, C., K. Yang, D. L. Farrens, Z. T. Farahbakhsh, H. G. Khorana, and W. L. Hubbell. 1996. Structural features and light-dependent changes in the cytoplasmic interhelical E-F loop region of rhodopsin: a site-directed spin-labeling study. *Biochemistry.* 35:12470–12478.

Baldwin, J. M. 1993. The probable arrangement of the helices in G protein-coupled receptors. *EMBO J.* 12:1693–1703.

Baldwin, J. M. 1994. Structure and function of receptors coupled to G proteins. *Curr. Opin. Cell. Biol.* 6:180–190.

Baldwin, M. J., G. F. X. Schertler, and V. M. Unger. 1997. An alpha-carbon template for the transmembrane helices in the rhodopsin family of G-protein-coupled receptors. *J. Mol. Biol.* 272:144–164.

Ballesteros, J., S. Kitanovic, F. Guarnieri, P. Davies, B. J. Fromme, K. Konvicka, L. Chi, R. P. Millar, J. S. Davidson, H. Weinstein, and S. C. Sealfon. 1998. Functional microdomains in G-protein-coupled receptors: the conserved arginine cage motif in the gonadotropin-releasing hormone receptor. *J. Biol. Chem.* 273:10445–10453.

Ballesteros, J. A., and H. Weinstein. 1992. The role of Pro/Hyp-kinks in determining the transmembrane helix length and gating mechanism of a [Leu]zervamicin channel. *Biophys. J.* 62:110–111.

Ballesteros, J. A., and H. Weinstein. 1995. Integrated methods for the construction of three-dimensional models and computational probing of structure-function relations in G protein-coupled receptors. *In* Methods in Neurosciences. Academic Press, San Diego, CA. 366–428.

Berlose, J. P., O. Convert, A. Brunissen, G. Chassaing, and S. Lavielle. 1994. Three-dimensional structure of the highly conserved seventh transmembrane domain of G-protein coupled receptors. *Eur. J. Biochem.* 225:827–843.

Bernstein, F. C., T. F. Koetzle, G. J. B. Williams, E. F. Meyer, M. D. Brice, J. R. Rodgers, O. Kennard, T. Shimanouchi, and M. Tasumi. 1977. The Protein Data Bank: a computer-based archival file for macromolecular structures. *J. Mol. Biol.* 112:535–542.

Birnbaumer, L., J. Abramowitz, and A. M. Brown. 1990. Receptor effector coupling by G-proteins. *Biochim. Biophys. Acta.* 1031:163–224.

Brooks, B. R., R. E. Bruccoleri, B. D. Olafson, D. J. States, S. Swaminathan, and M. Karplus. 1983. CHARMM: a program for macromolecular energy, minimization, and dynamics calculations. *J. Comp. Chem.* 4:187–217.

Clapham, D. E. 1996. The G-protein nanomachine. *Nature.* 379:297–299.

Colson, A., J. H. Perlman, A. Smolyar, M. C. Gershengorn, and R. Osman. 1998. Static and dynamic roles of extracellular loops in G-protein-coupled receptors: a mechanism for sequential binding of thyrotropin-releasing hormone to its receptor. *Biophys. J.* 74:1087–1100.

Dohlman, H. G., J. Thorner, M. G. Caron, and R. J. Lefkowitz. 1991. Model systems for the study of seven-transmembrane-segment receptors. *Annu. Rev. Biochem.* 60:653–688.

Donnelly, D., J. P. Overington, S. V. Ruffle, J. H. A. Nugent, and T. L. Blundell. 1993. Modelling alpha-helical transmembrane domains: the calculation and use of substitution tables for lipid-facing residues. *Protein Sci.* 2:55–70.

Elling, C. E., S. M. Nielsen, and T. W. Schwartz. 1995. Conversion of antagonist-binding site to metal-ion site in the tachykinin NK-1 receptor. *Nature.* 374:74–77.

Elling, C. E., and T. W. Schwartz. 1996. Connectivity and orientation of the seven helical bundle in the tachykinin NK-1 receptor probed by zinc site engineering. *EMBO J.* 15:6213–6219.

Farahbakhsh, Z. T., K. D. Ridge, H. G. Khorana, and W. L. Hubbell. 1995. Mapping light-dependent structural changes in the cytoplasmic loop connecting helices C and D in rhodopsin: a site-directed spin labeling study. *Biochemistry.* 34:8812–8819.

Farrens, D. L., C. Altenbach, K. Yang, W. L. Hubbell, and H. G. Khorana. 1996. Requirements of rigid-body motion of transmembrane helices for light activation of rhodopsin. *Science.* 274:768–770.

Findlay, J. B. C., D. Donnelly, N. Bhogal, C. Hurrell, and T. K. Atwood. 1993. Structure of G-protein-linked receptors. *Biochem. Soc. Trans.* 21:869–873.

Fu, D., J. A. Ballesteros, H. Weinstein, J. Chen, and J. A. Javitch. 1996. Residues in the seventh membrane-spanning segment of the dopamine D2 receptor accessible in the binding-site crevice. *Biochemistry.* 35: 11278–11285.

Gether, U., S. Lin, P. Ghanouni, J. A. Ballesteros, H. Weinstein, and B. K. Kobilka. 1997. Agonists induce conformational changes in transmembrane domains III and VI of the β_2 adrenergic receptor. *EMBO J.* 16:6737–6747.

Gether, U., S. Lin, and B. K. Kobilka. 1995. Fluorescent labeling of purified beta 2 adrenergic receptor. Evidence for ligand-specific conformational changes. *J. Biol. Chem.* 270:28268–28275.

Guarnieri, F., and H. Weinstein. 1996. Conformational memories and the exploration of biologically relevant peptide conformations: an illustration for the gonadotropin-releasing hormone. *J. Am. Chem. Soc.* 118: 5580–5589.

Guarnieri, F., and S. R. Wilson. 1995. Conformational memories and a simulated annealing program that learns. Application to LTB_4. *J. Comput. Chem.* 16:648–653.

Gudermann, T., T. Schoneberg, and G. Schultz. 1997. Functional and structural complexity of signal transduction via G-protein-coupled receptors. *Annu. Rev. Neurosci.* 20:399–427.

Hubbell, W. L., Z. T. Farahbakhsh, K. D. Ridge, K. Yang, D. Farrens, J. Resek, and H. G. Khorana. 1995. Exploring rhodopsin structure and dynamics with site-directed spin labeling. *Biophys. J.* 68:A21.

Hutchins, C. 1994. Three-dimensional models of the D1 and D2 dopamine receptors. *Endocr. J.* 2:7–23.

Javitch, J. A., D. Fu, and J. Chen. 1995. Residues in the fifth membrane-spanning segment of the dopamine D2 receptor exposed in the binding-site crevice. *Biochemistry.* 34:16433–16439.

Javitch, J. A., X. Li, J. Kaback, and A. Karlin. 1994. A cystine residue in the third membrane-spanning segment of the human D2 dopamine receptor is exposed in the binding-site crevice. *Proc. Natl. Acad. Sci. USA.* 91:10355–10359.

Laakkonen, L. J., F. Guarnieri, J. H. Perlman, M. C. Gershengorn, and R. Osman. 1996. A refined model of the thyrotropin-releasing hormone (TRH) receptor binding pocket. Novel mixed mode Monte Carlo/stochastic dynamics simulations of the complex between TRH and TRH receptor. *Biochemistry.* 35:7651–7663.

Liu, J., T. Schoneberg, M. Rhee, and J. Wess. 1995. Mutational analysis of the relative orientation of transmembrane helices I and VII in G protein-coupled receptors. *J. Biol. Chem.* 270:19532–19539.

Luo, X., D. Zhang, and H. Weinstein. 1994. Ligand-induced domain motion in the activation mechanism of a G-protein-coupled receptor. *Protein Eng.* 7:1441–1448.

MaloneyHuss, K., and T. P. Lybrand. 1992. Three-dimensional structure for the beta 2 adrenergic receptor protein based on computer modeling studies. *J. Mol. Biol.* 225:859–871.

McDonald, D. Q., and W. C. Still. 1992. AMBER* torsional parameters for the peptide backbone. *Tetrahedron Lett.* 33:7743–7746.

McDonald, I. K., and J. M. Thornton. 1994. Satisfying hydrogen bonding potential in proteins. *J. Mol. Biol.* 238:777–793.

Metropolis, N., A. W. Rosenbluth, M. N. Rosenbluth, A. H. Teller, and E. Teller. 1953. Equation of state calculation by fast computing machines. *J. Chem. Phys.* 21:1087–1092.

Mizobe, T., M. Maze, V. Lam, S. Suryanarayana, and B. K. Kobilka. 1996. Arrangement of transmembrane domains in adrenergic receptors. Similarity to bacteriorhodopsin. *J. Biol. Chem.* 271:2387–2389.

Mohamadi, F., N. G. J. Richards, W. C. Guida, R. Liskamp, M. Lipton, C. Caulfield, G. Chang, T. Hendrickson, and W. C. Still. 1990. An integrated software system for modeling organic and bioorganic molecules using molecular mechanisms. *J. Comput. Chem.* 11:440–467.

Oprian, D. D. 1992. The ligand-binding domain of rhodopsin and other G protein-linked receptors. *J. Bioenerg. Biomembr.* 24:211–217.

Perlman, J. H., A. O. Colson, W. Wang, K. Bence, R. Osman, and M. C. Gershengorn. 1997. Interactions between conserved residues in transmembrane helices 1, 2, and 7 of the thyrotropin-releasing hormone receptor. *J. Biol. Chem.* 272:11937–11942.

Pogozheva, I. D., A. L. Lomize, and H. I. Mosberg. 1997. The transmembrane 7-α-bundle of rhodopsin: distance geometry calculation with hydrogen bonding constraints. *Biophys. J.* 70:1963–1985.

Rao, V. R., G. B. Cohen, and D. D. Oprian. 1994. Rhodopsin mutation G90D and a molecular mechanism for congenital night blindness. *Nature.* 367:639–642.

Resek, J. F., Z. T. Farahbakhsh, W. L. Hubbell, and H. G. Khorana. 1993. Formation of the meta II photointermediate is accompanied by conformational changes in the cytoplasmic surface of rhodopsin. *Biochemistry.* 32:12025–12032.

Richardson, J. S., and D. C. Richardson. 1988. Amino acid preferences for specific locations at the ends of alpha helices. *Science.* 240:1648–1652 (erratum: *Science.* 242:1624).

Sankararamakrishnan, R., and S. Vishveshwara. 1992. Geometry of proline-containing alpha-helices in proteins. *Int. J. Pept. Protein Res.* 39: 356–363.

Schertler, G. F., and P. A. Hargrave. 1995. Projection structure of frog rhodopsin in two crystal forms. *Proc. Natl. Acad. Sci. USA.* 92: 11578–11582.

Schwartz, T. W. 1994. Locating ligand-binding sites in 7TM receptors by protein engineering. *Curr. Opin. Biotechnol.* 5:434–444.

Sealfon, S. C., L. Chi, B. J. Ebersole, V. Rodic, D. Zhang, J. A. Ballesteros, and H. Weinstein. 1995. Related contribution of specific helix 2 and 7 residues to conformational activation of the serotonin 5-HT2A receptor. *J. Biol. Chem.* 270:16683–16688.

Sheikh, S. P., T. A. Zvyaga, O. Lichtarge, T. P. Sakmar, and H. R. Bourne. 1996. Rhodopsin activation blocked by metal-ion-binding sites linking transmembrane helices C and F. *Nature.* 383:347–350.

Shenkin, P. S., and D. Q. McDonald. 1994. Cluster analysis of molecular conformations. *J. Comput. Chem.* 15:899–916.

Still, C. W., A. Tempczyk, R. C. Hawley, and T. Hendrickson. 1990. Semianalytical treatment of solvation for molecular mechanics and dynamics. *J. Am. Chem. Soc.* 112:6127–6129.

Strahs, D., and H. Weinstein. 1997. Comparative modeling and molecular dynamics studies of the δ, κ and μ opioid receptors. *Protein Eng.* 10:1019–1038.

Trumpp Kallmeyer, S., J. Hoflack, A. Bruinvels, and M. Hibert. 1992. Modeling of G-protein-coupled receptors: application to dopamine, adrenaline, serotonin, acetylcholine, and mammalian opsin receptors. *J. Med. Chem.* 35:3448–3462.

Turcatti, G., K. Nemeth, M. D. Edgerton, U. Meseth, F. Talabot, M. Peitsch, J. Knowles, H. Vogel, and A. Chollet. 1996. Probing the structure and function of the tachykinin neurokinin-2 receptor through biosynthetic incorporation of fluorescent amino acids at specific sites. *J. Biol. Chem.* 271:19991–19998.

Unger, V. M., P. A. Hargrave, J. M. Baldwin, and G. F. X. Schertler. 1997. Arrangement of rhodopsin transmembrane α-helices. *Nature.* 389: 203–206.

van Rhee, A. M., and K. A. Jacobson. 1996. Molecular architecture of G protein-coupled receptors. *Drug Dev. Res.* 37:1–38.

Wess, J., S. Nanavati, Z. Vogel, and R. Maggio. 1993. Functional role of proline and tryptophan residues highly conserved among G protein-coupled receptors studied by mutational analysis of the m3 muscarinic receptor. *EMBO J.* 12:331–338.

Wong, S. K., C. Slaughter, A. E. Ruoho, and E. M. Ross. 1988. The catecholamine binding site of the beta-adrenergic receptor is formed by juxtaposed membrane-spanning domains. *J. Biol. Chem.* 263: 7925–7928.

Yang, K., D. L. Farrens, W. L. Hubbell, and H. G. Khorana. 1996. Structure and function in rhodopsin. Single cysteine substitution mutants in the cytoplasmic interhelical E-F loop region show position-specific effects in transducin activation. *Biochemistry.* 35:12464–12469.

Yu, H., M. Kono, T. D. McKee, and D. D. Oprian. 1995. A general method for mapping tertiary contacts between amino acid residues in membrane-embedded proteins. *Biochemistry.* 34:14963–14969.

Zhang, D., and H. Weinstein. 1993. Signal transduction by a 5-HT2 receptor: a mechanistic hypothesis from molecular dynamics simulations of the three-dimensional model of the receptor complexed to ligands. *J. Med. Chem.* 36:934–938.

Zhang, D., and H. Weinstein. 1994. Polarity conserved positions in transmembrane domains of G-protein coupled receptors and bacteriorhodopsin. *FEBS Lett.* 337:207–212.

Zhou, W., C. Flanagan, J. A. Ballesteros, K. Konvicka, J. S. Davidson, H. Weinstein, R. P. Millar, and S. C. Sealfon. 1994. A reciprocal mutation supports helix 2 and helix 7 proximity in the gonadotropin-releasing hormone receptor. *Mol. Pharmacol.* 45:165–170.